Supporting Information

Enhanced Performance of Single-crystal Perovskite Solar cells via In-situ Passivation of Ionic-Liquid

Tongpeng Zhao,[1#] Ruiqin He,[1#] Yuxin Gao,[1] Chunmei Wang,[1] De Yu,[1] Xuesong Liu,[1] Tanghao Liu,[2*] Yimu Chen[1*]

[1]School of Integrated Circuits, Harbin Institute of Technology (Shenzhen), Shenzhen, Guangdong 518055, China

[2]School of Physical Sciences, Great Bay University, Dongguan, Guangdong 523000, China

[#]These authors contributed equally to this work.

[*]Corresponding authors: Yimi Chen (email: chenyimu@hit.edu.cn), Tanghao Liu (email: tanghaoliu@gbu.edu.cn)

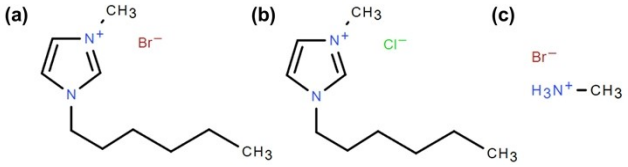

Figure S1. Molecular structure of (a) HMIMBr, (b) HMIMCl and (c) MABr.

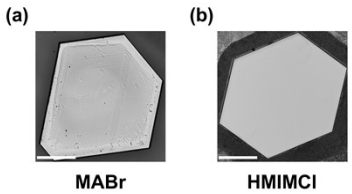

Figure S2. Optical microscope images of SCTFs with (a) MABr and (b) HMIMCl (Scale bar: 500 μm).

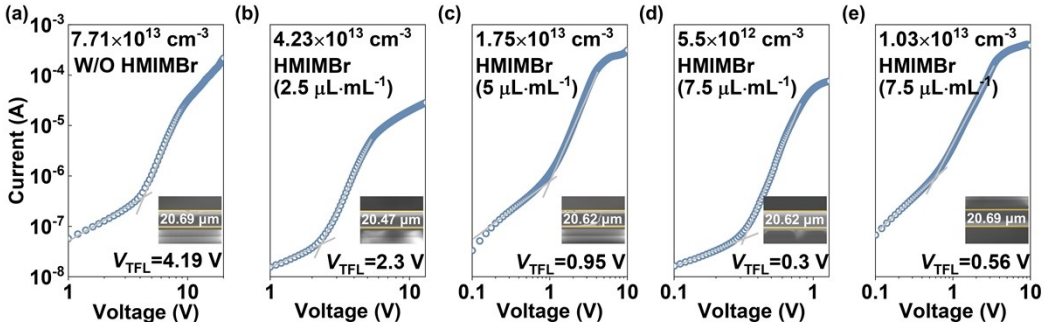

Figure S3. SCLC measures of SCTF devices based on the different HMIMBr concentration (The inset shows the sample thickness characterized by SEM).

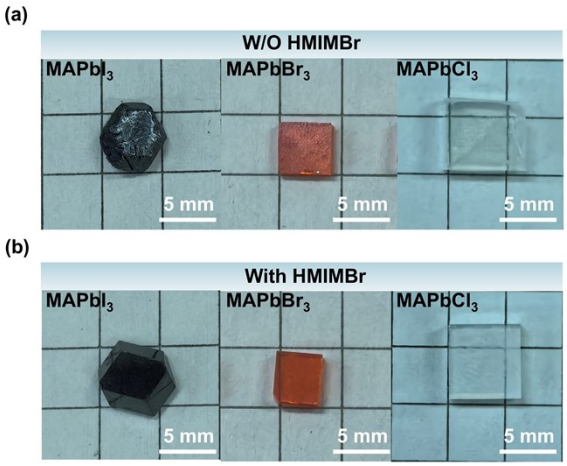

Figure S4. Comparison of the growth morphologies of bulk SCs (a) without and (b) with HMIMBr modification.

(a)

Map W/O HMIMBr

Element	Mass Norm. [%]	Atom [%]
Br	0.00	0.00
I	59.82	70.86
Pb	40.18	29.14
	100.00	**100.00**

(b)

Map With HMIMBr

Element	Mass Norm. [%]	Atom [%]
Br	0.18	0.32
I	65.54	75.49
Pb	34.28	24.18
	100.00	**100.00**

Figure S5. EDS mapping elemental composition analysis of SCTFs (a) without and (b) with HMIMBr modification.

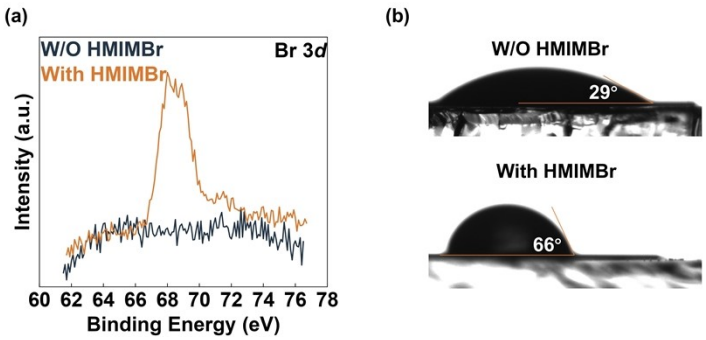

Figure S6. (a) Br 3*d* XPS spectra of SCTFs and (b) Contact angle of water solution on the SCTFs surface without and with HMIMBr modification.

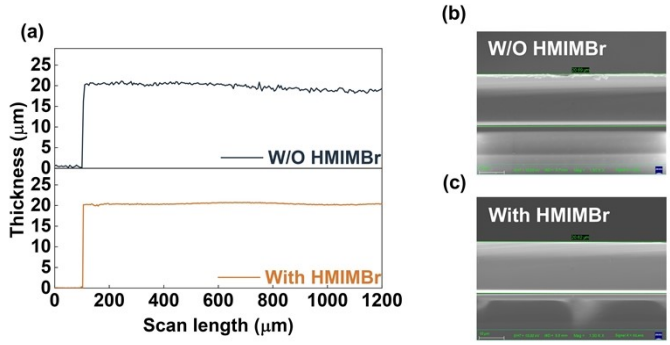

Figure S7. (a) The step profiler curves and cross-sectional SEM images of SCTFs (b) without and (c) with HMIMBr modification.

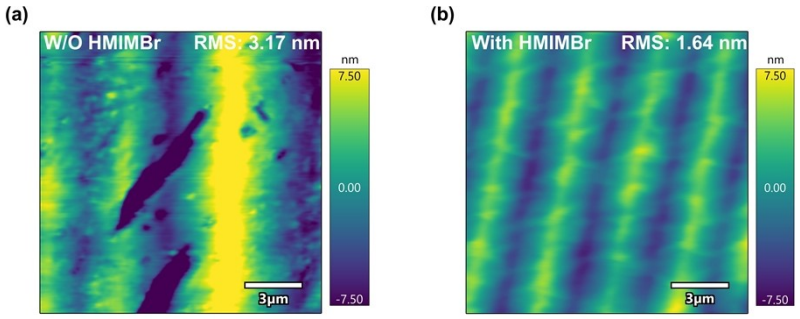

Figure S8. AFM images of SCTFs surface (a) without and (b) with HMIMBr modification.

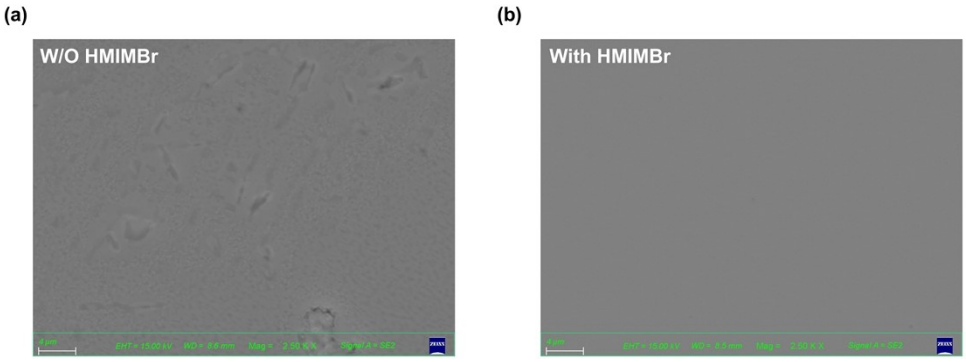

Figure S9. Surface SEM images of SCTFs (a) without and (b) with HMIMBr modification.

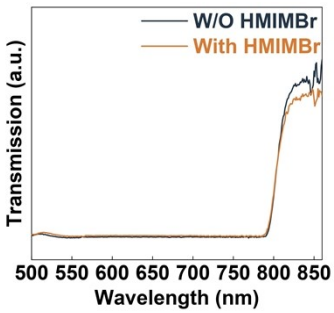

Figure S10. Transmission spectra of SCTFs without and with HMIMBr modification.

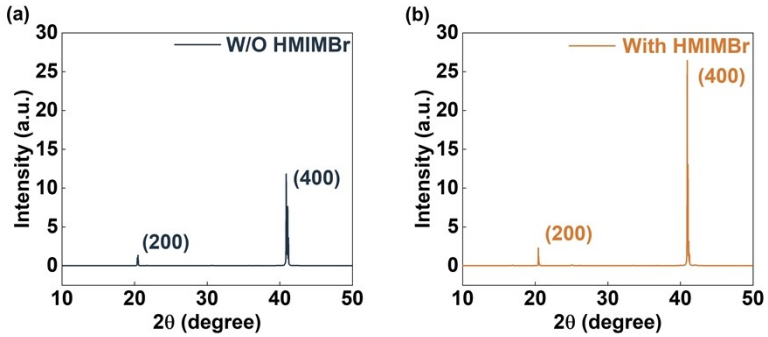

Figure S11. XRD measures of SCTFs (a) without and (b) with HMIMBr modification.

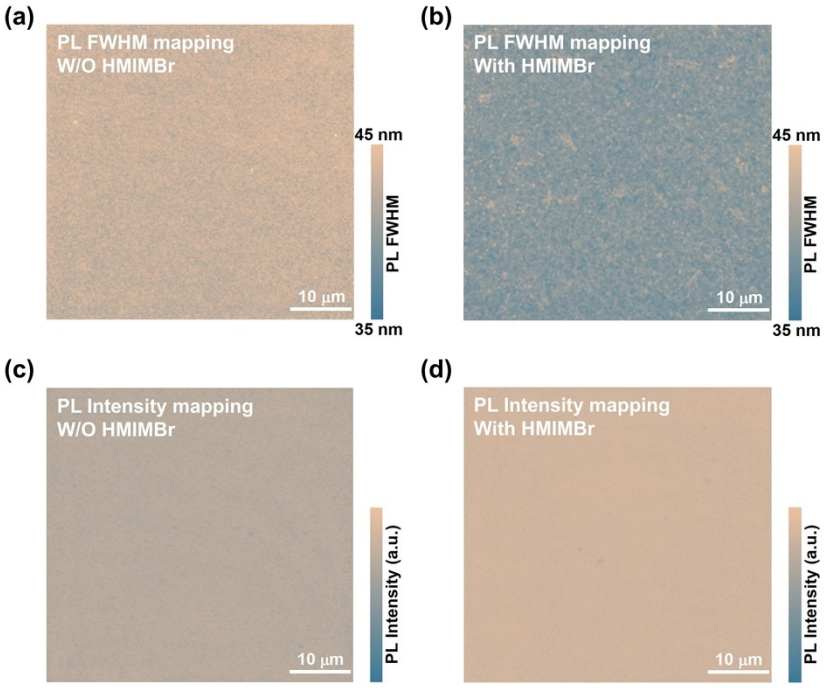

Figure S12. (a-b) PL FWHM mapping and (c-d) PL Intensity mapping of SCTFs without and with HMIMBr modification.

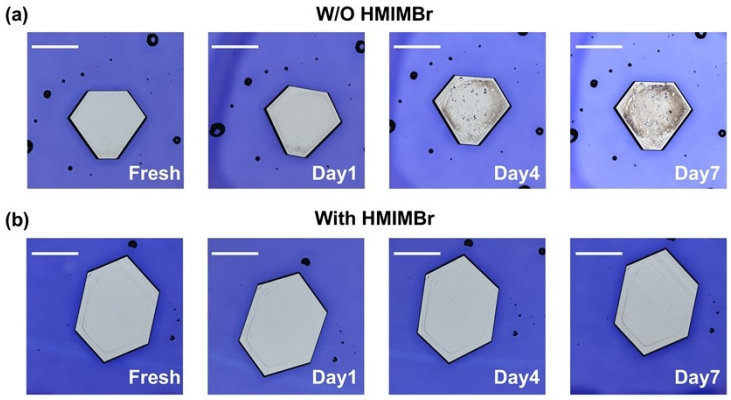

Figure S13. Optical microscope images of SCTFs (a) without and (b) with HMIMBr modification (Scale bar: 500 μm).

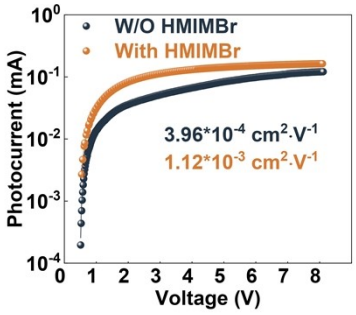

Figure S14. Photoconductivity measurements of SCTF devices without and with HMIMBr modification.

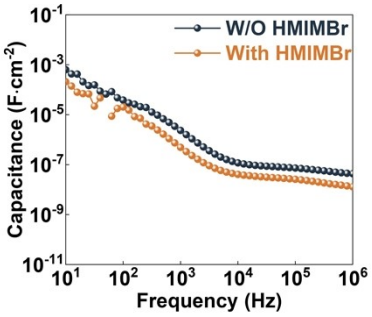

Figure S15. C-*f* measurements of SCTF devices without and with HMIMBr modification.

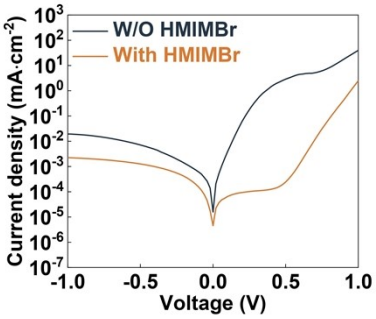

Figure S16. Dark *J-V* curves of SCTF devices without and with HMIMBr modification.

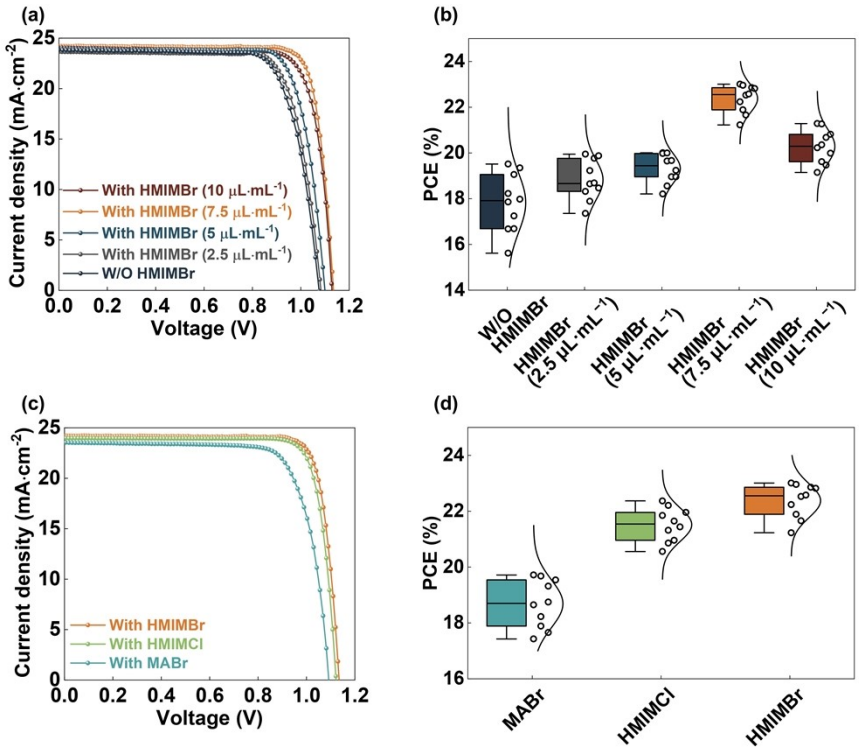

Figure S17. (a) The champion PCE curves and (b) Statistical PCE data of SCTF devices based on the different HMIMBr concentration; (c) The champion PCE curves and (d) Statistical PCE data of SCTF devices based on the different additives.

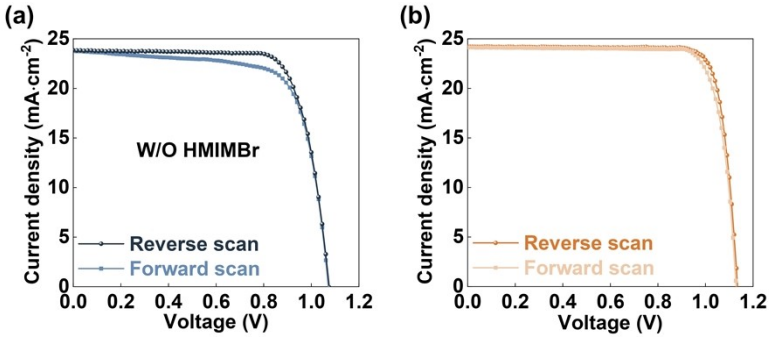

Figure S18. Forward and reverse *J-V* curves of SCTF devices (a) without and (b) with HMIMBr modification.

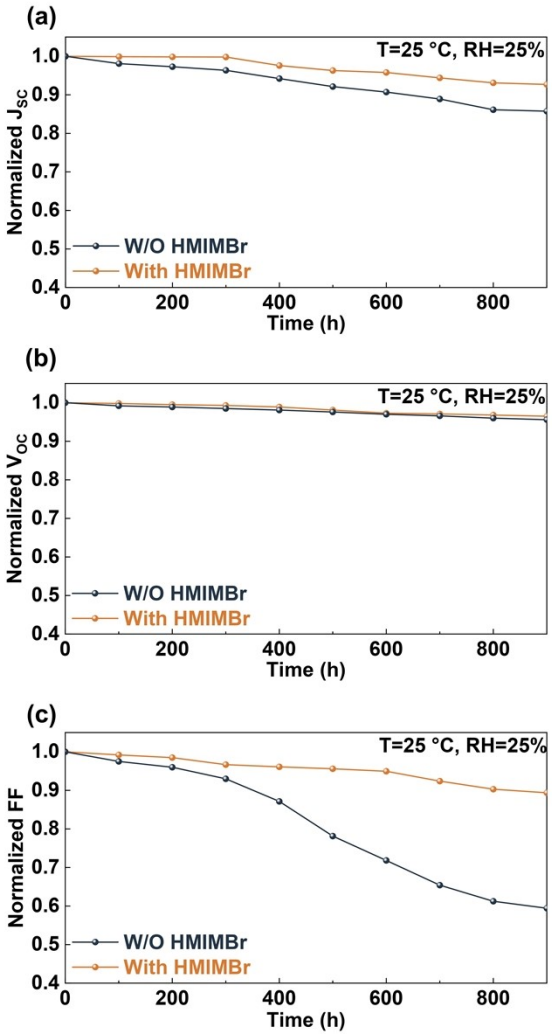

Figure S19. Long-term storage stability of SCTF devices without and with HMIMBr modification, including normalized (a) *J*sc, (b) *V*oc and (c) FF,

Table S1. Parameters of $MAPbI_3$ SCTF champion devices with the different HMIMBr doping concentrations

	J_{SC} (mA·cm^2)	V_{OC} (V)	FF (%)	PCE (%)
W/O HMIMBr	23.84	1.07	76.52	19.52
HMIMBr (2.5 μL·mL^{-1})	23.64	1.083	77.92	19.95
HMIMBr (5 μL·mL^{-1})	23.92	1.10	79.84	21.01
HMIMBr (7.5 μL·mL^{-1})	24.21	1.135	83.73	23.01
HMIMBr (10 μL·mL^{-1})	24.06	1.128	80.76	21.92

Table S2. Parameters of $MAPbI_3$ SCTF champion devices with the different additives

	J_{SC} (mA·cm^2)	V_{OC} (V)	FF (%)	PCE (%)
MABr	23.54	1.09	76.86	19.72
HMIMCl	23.98	1.122	83.14	22.37
HMIMBr	24.21	1.135	83.73	23.01

Table S3. Statistical parameters of *J-V* characteristics under applied bias for $MAPbI_3$ SCTF devices with HMIMBr modification

	J_{SC} (mA·cm^2)	V_{OC} (V)	FF (%)	PCE (%)
Initial	24.19	1.12	80.79	21.89
-1 V (40 s)	23.81	1.09	79.72	20.69
-1 V (80 s)	23.32	1.06	75.69	18.71
-1 V (120 s)	22.45	1.03	71.79	16.60

Table S4. Statistical parameters of *J-V* characteristics under applied bias for $MAPbI_3$ SCTF devices without HMIMBr modification

	J_{SC} (mA·cm^2)	V_{OC} (V)	FF (%)	PCE (%)
Initial	23.86	1.07	75.79	19.35
-1 V (40 s)	23.27	1.05	70.55	17.24
-1 V (80 s)	22.39	1.01	65.62	14.84
-1 V (120 s)	21.59	0.98	50.71	10.73

Table S5. Device parameter attenuation data with HMIMBr modification

	J_{SC} (mA·cm^2)	V_{OC} (V)	FF (%)	PCE (%)
Initial	24.20	1.13	81.33	22.24
300 h	24.18	1.12	78.73	21.32
600 h	23.16	1.09	77.96	19.68
900 h	22.36	1.09	73.07	17.81

Table S6. Device parameter attenuation data without HMIMBr modification

	J_{SC} (mA·cm^2)	V_{OC} (V)	FF (%)	PCE (%)
Initial	23.60	1.07	75.48	19.06
300 h	22.73	1.05	72.53	17.31
600 h	21.40	1.04	54.14	12.05
900 h	20.24	0.79	42.30	6.76

Supplementary Note 1.

The host halogen component of the perovskite adopted in this work is iodine. The Pb-Br bond exhibits higher bond energy than the Pb-I bond, enabling Br-containing ionic liquids to achieve superior surface passivation and coverage protection on SCTF surfaces. Although the Pb-Cl bond has a stronger bond energy than the Pb-Br bond, the considerable difference in bond length between Pb-Cl and Pb-I results in lattice mismatch between the surface and bulk of the single-crystal, which further induces surface stress and lattice distortion[1]. The modification of perovskite photovoltaic devices by ionic liquids with different halogen atoms has been reported in previous literature, where ionic liquids Br-containing are proven to deliver the optimal surface passivation performance[2, 3]. This conclusion is also well verified by our device efficiency data presented in Figure S17c, S17d and Table S2. Accordingly, HMIMBr is selected as the primary research object in this study.

1. S. Han, L. Guan, T. Yin, J. Zhang, J. Guo, X. Chen and X. Li, *Phys. Chem. Chem. Phys.*, 2022, **24**, 10184-10192.
2. R. García-Rodríguez, D. Ferdani, S. Pering, P. J. Baker and P. J. Cameron, *J. Mater. Chem. A*, 2019, **7**, 22604-22614.
3. Z. Chen, S. Jiang, Z. Liu, Y. Li, J. Shi, H. Wu, Y. Luo, D. Li and Q. Meng, *J. Mater. Chem. A*, 2024, **12**, 16070-16078.